Cement and Concrete Research 120 (2019) 217–226

Contents lists available at ScienceDirect

Cement and Concrete Research

journal homepage: www.elsevier.com/locate/cemconres

Rheological behaviors and model of fresh concrete in vibrated state

Zhuguo Li*, Guodong Cao

School of Science and Technology for Innovation, Yamaguchi University, Ube, Yamaguchi, Japan

ARTICLE INFO

Keywords:
Fresh concrete
Rheological model
Vibration
Vibration damping
Oscillatory rheometer

ABSTRACT

The rheological behavior of fresh concrete under vibration is very different from that in static state. In this study, the relationship between shear strain rate and shear stress of fresh concrete under vibration was theoretically analyzed based on Eyring rate process theory and vibration damping theory, and the constitutive equations were gotten. At low shear strain rates, vibrated fresh concrete is a Bingham liquid, even Newtonian when vibrating time is enough long. However, at high shear strain rates, the shear stress - shear strain rate relationship is a logarithmic function. The shear deformation resistance decreases with increasing vibrating time, but increases with the distance from vibrator or the thickness of concrete. The rheological measurement in vibrated state was also conducted by using a ring shear type rheometer, into which a rod vibrator is integrated. The experimental results of shear stress - shear strain rate relationship were well consistent with the theoretical equations.

1. Introduction

With the advance of computer technology, numerical flow simulation becomes possible to evaluate and design workability of fresh concrete, with taking structural conditions and construction method into account. So far, many numerical methods and simulation examples, generally using Bingham model as the constitutive model, are associated with self-compacting concrete (SCC) that flows under its gravity. However, SCC has not yet widely used on construction site, vibration is still in widespread use. During the casting process, vibration would help to release entrapped air and to cast concrete into formwork fully [1]. But slight vibration doesn't work well, excessive vibration may result in segregation so that honeycombs are caused [2].

The rheological behavior of fresh concrete under vibration is different from that in static state. However, the concrete at a greater distance from vibrator is unaffected. The radius of action of vibrator is dependent on the frequency (f) and amplitude (S) of vibration for a given acceleration ($\propto Sf^2$), and a vibrator with high amplitude is more effective than one with low amplitude but higher frequency [3]. Banfill et al. confirmed the importance of peak velocity ($\propto f\ S$) as the most important characteristic of vibration governing efficacy, the radius of action increases with increasing the peak velocity [4]. Besides the characteristics of vibrator, the rheological properties of fresh concrete also affect the radius of action of rod vibrator. The radius of action increases with decreasing yield stress and with increasing plastic viscosity [4]. Hence, only based on the slump that is a test result in static state, it is difficult to predict the filling ability in mould under vibration. The experimental evaluation of filling ability and degree of fresh concrete under vibration is certainly a time-consuming job. Numerical flow simulation is an alternative approach to the experiment evaluation. Unfortunately, there are few studies on flow simulation of vibrated concrete. One reason is that constitutive model of vibrated fresh concrete has not yet established now.

Mori and Tanigawa have proposed a flow simulation method of fresh concrete under vibration based on visco-plastic finite element analysis [5]. As application of vibrating force, vibrating acceleration is introduced as nodal force, which is reversed reciprocally step by step. And this simulation method treats fresh concrete under vibration with the Bingham model that has smaller yield value and plastic viscosity than the same concrete in unvibrated state. Large forces act in momentary time, and some elements of fresh concrete yield and flow.

There is no doubt that fresh concrete is a special granular material containing water, not an absolute suspension. The inter-particle friction and the inter-particle contact angle (see Fig. 1) result in part of shear deformation resistance [6]. Viscous resistance is another source of shear deformation resistance. Basically, vibratory consolidation of granular materials is achieved by the motion of particles due to vibration force and decrease of inter-particle friction. L'Hermite and Tournon have shown that the internal friction in fresh concrete during vibration is reduced to about 5% of the value at rest [7]. Moreover, vibration makes mean particle contact angle of granular body decrease after an instant increase in the beginning of vibration due to the precipitation of suspended particles [8]. Hence, concrete mixture of normal consistencies behaves like a fluid during vibration [9]. Application of vibration

* Corresponding author.
E-mail address: li@yamaguchi-u.ac.jp (Z. Li).

https://doi.org/10.1016/j.cemconres.2019.03.020
Received 29 April 2018; Received in revised form 12 March 2019; Accepted 15 March 2019

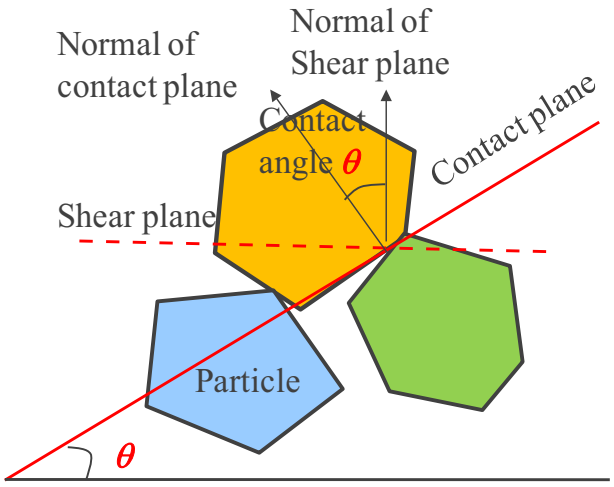

Fig. 1. Concept of particle contact angle.

reduces the yield value markedly, and at least to an extent such that fresh concrete can flow under its own weight [10].

Tattersall and Baker [10] measured the rheological properties of vibrated fresh concrete with the impeller rheometer, of which the bowl was mounted on a vibrating table. The results show that when vibration is applied to fresh concrete, the flow properties are no longer represented by the simple linear Bingham model, but approximate to those of a power law pseudoplastic with zero yield value, and that the effectiveness of the vibration is to be assessed in terms of its maximum velocity. They further confirmed that, using a vertical pipe apparatus placed on a vibrating table, at low shear strain rates of the order of those prevailing in many practical circumstances, fresh concrete under vibration behaves as a Newtonian liquid, which explains why it would flow under self-weight [11].

Teranishi et al. [12] performed the sphere lifting test of fresh mortar under vibration, placing sample container on a table vibrator. They found that, in the range of low shear strain rate, the consistency of Bingham fluid under vibration was a curve through the origin, but apparent viscosity increased in comparison with the same concrete in unvibrated state.

However, Hu and Larrard [13] disagreed to the Tallersall and Baker's conclusions stated above. They measured the flow curves of the concretes (slump value over 10 cm) under vibration with the BTRHEOM rheometer, of which the sample container was placed on a vibrating plate with frequency of 50 Hz and acceleration of 4 g, and found that the concretes under vibration remained Binghamian. Compared with the measurement without vibration, the yield stress was reduced about 50%. However, the plastic viscosity was little influenced, and even increased for the low-viscosity concretes.

The above experimental investigations didn't give consistent conclusion, and had the same feature that vibrating force was applied in vertical direction, the vibration of practical rod vibrator is however horizontal. Moreover, the vibration is attenuated along the distance from vibrating source. The liquefaction, i.e. the particles in concrete become separated, of fresh concrete under vibration needs time. Hence, the experimental result of the consistency under vibration is greatly affected by the consistency in unvibrated state, the position of measured concrete sample from vibrator, and the elapsed time of vibration before measurement. However, the test conditions of the above investigations were not clear.

Li clarified the flow mechanism of fresh concrete under a shear stress by expanding the viscosity theory of Eyring rate process, and further investigated the consistency equation of high fluidity concrete without the consideration of shear deformation resistance caused by particle contact angle θ (θ is also related to dilatancy) but inter-frictional angle [14], and the rheological model (briefly called VGM model) of common fresh concrete in static state considering the particle contact angle and its change with shearing time besides the inter-frictional angle [15]. The nonlinear VGM model can describe the normal stress and shearing time-dependence of rheological properties of fresh concrete, thus yields more precise flow simulation than the Bingham model [16]. Li also developed a rheometer (called RSNS rheometer) for flowing concrete (slump is over 12 cm), of which mechanism is the same to the BTRHEOM rheometer. The ring-shaped concrete around a central axis is sheared between two horizontal blades. However, the central axis is the head of rod vibrator, and the RSNS rheometer can measure no matter under stress growth control or under shear strain rate growth control, and the normal stress acting on the shear plane can be freely adjusted by two air cylinders [15].

In this study, a theoretical analysis of consistency of fresh concrete under vibration was first conducted based on the Eyring rate process theory. The effects of vibrating time, distance from vibrating source, slump, and concrete thickness on the shear deformation resistance of fresh concrete under vibration were discussed. Then the shear stress-shear strain/shear strain rate relationship of fresh mortar and concrete under vibrated were investigated by using the RSNS rheometer. The experimental and theoretical results were compared, and a rheological model was proposed for fresh concrete in vibrated state.

2. Theoretical analysis of rheological model under vibration

2.1. Basic consistency equation

The shear strain rate ($\dot{\gamma}$) of fresh concrete depends on the movement of the cement particles, and is expressed by Eq. (1) [14].

$$\dot{\gamma} = N_{ca} \cdot P_c \cdot \Lambda_c \cdot \cos\theta_c \tag{1}$$

where N_{ca} is number of potential active particle (hereafter called PA-particle), Λ_c is mean moving distance of cement particles till reaching to each stable position, θ_c is mean contact angle of moving cement particles, and P_c is the probability that PA-particles become moving cement particles in unit time, which is expressed by the first equation in Eq. (2).

$$P_c = 2A \sinh\left(\frac{f_v \cdot \Lambda_c}{2kT}\right), \quad A = \frac{kT}{p} \exp\left(-\frac{E_c}{kT}\right) \tag{2}$$

where T is absolute temperature (k), k is Boltzmann's constant (1.380662×10^{-23} J/k), p is Planck's constant ($6.6260755 \times 10^{-34}$ J·s), E_c is mean potential energy of cement particles (J), and f_v is mean shear force used to match viscous resistance imposed on a PA-particle, and is given by

$$f_v = (\tau_c - \tau_{cfd})/N_{ca} \tag{3}$$

where τ_c is shear stress imposed to all cement particles, τ_{cfd} is the shear stress used to match the frictional resistance and dilatancy-caused resistance of cement particles.

Only when the inter-particle force angle β of particle is greater than the sum of inter-particle frictional angle and particle contact angle, the particle becomes PA-particle. Since aggregate particle is not subjected to viscous resistance, PA-aggregate particle is moving particle. But for cement particle, only when the inter-particle force is so large that the viscous resistance of the PA-particle can be also matched, the PA-cement particle will become a moving cement particle [17]. In vibrated state, because inter-particle frictional angle and particle contact angle decrease, all the cement particles can be approximately regarded as PA-particle, i.e. $N_{ca} \fallingdotseq N_c$. N_c is total number of cement particles.

Moreover, moving distances of cement particles till they reach their stable positions, where the moving resistance (the sum of frictional, dilatancy-caused, and viscous resistances) is in balance with its subjected inter-particle force, are different individually. At present we suppose mean moving distance of cement particles (Λ_c) is a constant,

not changing with shear strain or shear strain rate of fresh concrete, and the θ_c.

If supposing that shear stress (τ_c) imposed on all cement particles is proportional to the volume ratio of cement particles to all solid particles, τ_c is expressed by Eq. (4) when a shear stress (τ) is applied to fresh concrete.

$$\tau_c = \frac{V_c}{V_c + V_a}\cdot\tau = S_d\tau \tag{4}$$

where V_c, V_a are volumes of cement particles and aggregate particles in unit volume of concrete, respectively (m^3/m^3); and S_d is stress distribution coefficient ($=V_c/(V_c+V_a)$).

The shear deformation resistance (τ_{fd}) of fresh concrete, caused by the inter-friction, the dilatancy-caused resistance, and the surface tension and suction effect of mixing water, is expressed by Eq. (5) [6,18].

$$\tau_{fd} = \sigma_n \tan(\phi + \theta) + C_w \tag{5}$$

where σ_n is normal stress acting on the shear plane, ϕ and θ are inter-frictional angle and mean particle contact angle of fresh concrete, respectively, and C_w is a resistance caused by mixing water.

According to Eq. (4), the shear deformation resistance (τ_{cfd}) of cement particles caused by the inter-friction, the dilatancy-caused resistance, and the surface tension and suction effect of mixing water, should be expressed as

$$\tau_{cfd} = S_d\cdot\tau_{fd} \tag{6}$$

Eq. (1) expresses that cement particles' movement causes a shear strain rate of fresh concrete, and shear strain rate depends on the number of moving cement particles and mean moving direction angle, i.e. mean particle contact angle. Because cement particles are tiny, it is considered that the effect of their mean moving direction angle on the shear strain rate is very small, compared to their number. Though in vibrated state, with the separation of flocculated cement particles, mean particle contact angle (θ_c) of moving cement particles becomes small, we approximated that the θ_c doesn't change with vibration time in this study.

Substituting Eqs. (2), (3), (4) and (6) into Eq. (1), the shear strain rate of fresh concrete under vibration is obtained as

$$\dot{\gamma} = 2A\cdot N_c\cdot\Lambda_c\cdot\cos\theta_c\cdot\sinh[c_2(\tau-\tau_{fd})] \tag{7}$$

where $c_2 = S_d\Lambda_c/2kTN_c$

As shown in Fig. 2, when $x \leqq 1$, the value of shin(x) is almost equal to x, and when $x > 1$, the value of exp(x) is very near to that of 2sinh (x). Hence, Eq. (7) can be simplified as Eqs. (8) and (9). At low shear strain rates, the shear stress - shear strain rate relationship is linear, but at high shear strain rates, the shear strain rate is an exponential function of shear stress.

$$\tau \approx \tau_{fd} + \eta\dot{\gamma},\quad \eta = \frac{p}{S_d\Lambda_c^2}\cdot\exp\left(\frac{E_c}{kT}\right)\cdot\cos\theta_c, \tag{8}$$

when $c_2(\tau-\tau_{fd}) \leqq 1$

$$\dot{\gamma} \approx A\cdot N_c\cdot\Lambda_c\cdot\cos\theta_c\cdot\exp[c_2(\tau-\tau_{fd})], \tag{9}$$

when $c_2(\tau-\tau_{fd}) > 1$

In vibrated state, with the separation of flocculated cement particles, their mean particle contact angle (θ_c) becomes small. Hence, the plastic viscosity η increases with the decrease of the θ_c.

Eq. (9) is rewritten in form of shear deformation resistance as shown in Eq. (10).

$$\tau = \tau_{fd} - \frac{1}{c_2}\ln(A\cdot N_c\cdot\Lambda_c\cdot\cos\theta_c) + \frac{1}{c_2}\ln\dot{\gamma} \tag{10}$$

Since the value of A is very small, Eq. (10) can be approximated as a logarithmic function.

$$\tau \approx \tau_{fd} + \frac{1}{c_2}\ln\dot{\gamma} \tag{11}$$

when $c_2(\tau-\tau_{fd}) > 1$

2.2. Effects of vibrating energy and time

In vibrated state, the inter-frictional angle is dynamic frictional angle. The liquefaction degree changes with vibrating time, thus the mean inter-frictional angle and the mean particle contact angle of fresh concrete vary with vibrating time.

Li and Tanigawa [8] performed the internal visualization experiments based on LAT (Laser-Aided Tomography) to investigate the variation of mean particle contact angle (θ) of granular material with vibrating time (t). The used granular materials were the mixtures of irregularly-shaped or round-shaped glass particles and silicon oil. Because the refractive indexes of the glass particle and the silicon oil were the same, the contours of glass particles in the silicon oil could be seen under the irradiation of green laser light.

The dynamic viscosity of the silicon oil was 20.6 cSt at 25 °C. The glass particles were first filled into a box without consolidation, which was made of transparent acrylic resin, and then they poured the silicon oil into the box till the top surface of glass particle assembly. The volume concentrations of glass particles were different from the mixtures, ranging from 54% to 58%. While the vibration was applied to the particle-viscous fluid systems by a rod vibrator, the photographs were taken for recording the change of internal situation of the systems with the vibrating time t. After analyzing the photographs, the $\theta - t$ relationship was examined. The details can be found in Reference [8, 19]. The conceptual diagram of obtained $\theta - t$ relationship is shown in

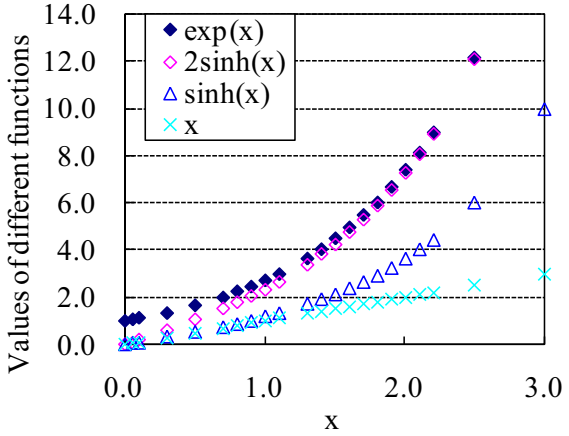

Fig. 2. Comparison of hyperbolic function with other functions.

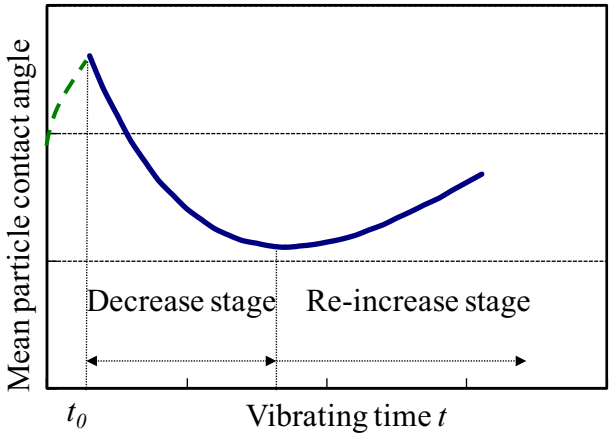

Fig. 3. Variation of mean particle angle with vibrating time.

Table 1
Parameters values of rheological model under vibration.

Series no.	σ_n (Pa)	ϕ_0 (rad)	θ_0 (rad)	c_3 (10^{-5})	ρ (kg/m^3)	S (mm)	f (Hz)	S_d	Λ_c (10^{-12} m)	N_c (10^{11})
1	2944	0.50	0.64	8	2403	1.8	220	0.322	8.0	1.79
2	2818	0.30	0.34	8	2300	1.8	220	0.350	8.5	1.40

	E_c (kT)	T (k)	θ_c (rad)	η (Pa·s)	t_0 (s)	$\Delta\tau$ (Pa/s)	ξ_m	ξ_B	n	m_v (kg)	m_b (kg)
1	29.5	293	0.20	204	0	50	0.04	0.9	0.5	1.21	0.37
2	29.2	293	0.15	145	0	50	–	–	–	–	–

[Notes] ρ is bulk density of fresh concrete, $\Delta\tau$ is increasing speed of shear stress, and t_0 is elapsed time of vibration before rheological measurement.

Fig. 3.

Immediately after the vibration is applied to the particle-viscous fluid systems, an abrupt increase of the θ was found. This is because the system was loose in the beginning so that the vibration caused slight precipitation of the particles. But continue vibration caused a decrease of the θ, and then a re-increase with the vibrating time. The decrease of the θ was because the particles move under the vibration so that the particles' contact became loose. But excessively loosening resulted in that the particles' own weight couldn't be supported so that part of the particles precipitated and contacted with others. For the reason, the re-increase of θ occurred after a long time of vibration.

However, fresh concrete is high viscous material, the first increase of θ doesn't occurs. And the re-increase wouldn't occur in actual concrete work because excessive vibration is not permitted for avoiding the segregation of fresh concrete. Hence, it is enough to consider only the decrease stage of θ for fresh concrete.

During vibration, not only the mean particle contact changes, but also the mean inter-particle angle (ϕ) changes with vibrating time since the particle contacts decrease gradually. But at present, it is difficult to measure the change of ϕ. Because the ϕ relates to the particle contact like as the mean particle contact angle, the looser the particle contacts in fresh concrete, the smaller the ϕ. Here we assumed that the change of ϕ is the same to the θ. And the liquefaction is essentially related to vibration energy. Therefore, in this study we supposed the relationship between the value of ($\phi + \theta$) and vibration energy as shown in Eq.(12). Moreover, in vibrated state, the movement of mixing water results in a reduction of wetting angle, the surface tension of water decreases. Hence, in this study, we ignore the C_w that is a shear deformation resistance caused by the surface tension and suction effect of water between solid particles.

$$\phi + \theta = (\phi_0 + \theta_0)\cdot[1 - (1 - \exp(-c_3 \cdot E))] \tag{12}$$

where ϕ_0, θ_0 are respectively initial values of mean inter-particle frictional angle and mean particle contact angle, c_3 is a constant for a given concrete, and E is vibration energy applied to concrete of unit volume (erg·s/cm^3).

E is expressed by Eq. (13) [20].

$$E = \rho\pi^2 S^2 f^2 t \tag{13}$$

where ρ is bulk density (g/cm^3), S is amplitude (cm), and f is frequency (Hz).

Based on Eqs. (5), (12) and (13), Eqs. (8) and (11) are transformed as

$$\tau = \sigma_n \tan\{(\phi_0 + \theta_0)[1 - (1 - \exp(-c_3\rho\pi^2 S^2 f^2 t))]\} + \eta\dot{\gamma} \tag{14}$$

when $c_2(\tau - \tau_{fd}) \leqq 1$

$$\tau = \sigma_n \tan\{(\varphi_0 + \theta_0)[1 - (1 - \exp(-c_3\rho\pi^2 S^2 f^2 t))]\} + \frac{1}{c_2}\ln\dot{\gamma} \tag{15}$$

when $c_2(\tau - \tau_{fd}) > 1$

With the increase of vibrating time for a given vibrator, the first terms in the right of Eqs. (14) and (15) decrease. Hence, the longer the vibrating time, the smaller the shear deformation resistance. When the vibrating time is short, the vibrated concrete behaves as Bingham fluid, but when the vibrating time is enough long, the vibrated concrete becomes to be a Newtonian liquid at low shear strain rates, as found in the experiments by Tattersall and Baker [7]. Because the decrease of the first term in the Eq. (14), the apparent viscosity of vibrated concrete increases with the vibrating time for a given shear strain rate, which agree with the results shown in References [12, 13].

At high shear strain rates, when the vibrating time is enough long, the $\dot{\gamma} - \tau$ relationship is an exponential curve similar to a Power Law curve, as found by Tattersall [10,12].

The value of c_2 varies with concrete mixture. According to the trail calculation shown in Ref. [21], c_2 is in range of 1.5–2.5 × 10^{-3}. Considering the τ_{fd} is small under vibration, the limit shear stress τ for dividing the straight and curved lines is within 1000 Pa, generally 400–700 Pa.

Based on the parameter values shown in Table 1 for two series of concrete mixtures with different fluidity. The higher the fluidity, the smaller the ϕ, and the θ, but the larger the S_d. The shear strain rate $\dot{\gamma}$ - shear stress τ relational curves of fresh concrete near a vibrator (x = 10 cm) and at the depth (h) of 25 cm are obtained according to Eqs. (14) and (15), as shown in Figs. 4–6.

Fig. 4 shows the effects of the increasing speed of shear stress ($\Delta\tau$, Pa/s) and the elapsed time (t_0, second) of vibration before the rheological measurement on the $\dot{\gamma}$ - τ relational curves of concrete mixture No. 1. During the rheological measurement, the vibration is continued, thus the vibrating time increases with the measuring time. As shown in Fig. 4, the greater the t_0, the larger the corresponding shear strain rate for a given shear stress. And for the same shear stress and the t_0, the shear strain rate $\dot{\gamma}$ measured under a greater shear stress speed $\Delta\tau$ is less than that measured under a smaller $\Delta\tau$. When the vibrating time before the rheological measurement is long, the yield stress nears zero.

Fig. 5 shows the effect of the fluidity of fresh concrete on the $\dot{\gamma}$ - τ relational curve under vibration. For the same vibration and rheological measurement conditions, Series No. 2 with higher fluidity has greater shear rates than Series No. 1, and the yield stress of No. 2 is smaller.

Fig. 6 shows the $\dot{\gamma}$ - τ relational curves of concrete mixture No. 1 at

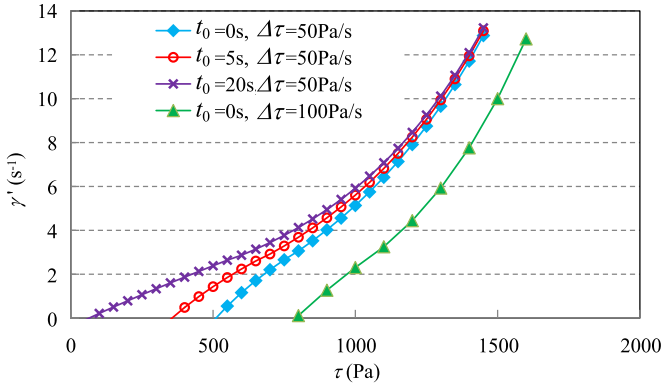

Fig. 4. Flow curves of vibrated concrete (No. 1) at different vibrating times.

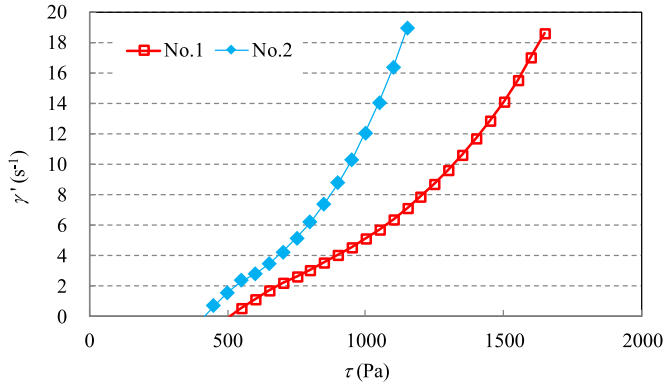

Fig. 5. The $\dot{\gamma}$ - τ relational curve of fresh concrete with different slump (t_0 = 0 s, $\Delta\tau$ = 50 Pa/s).

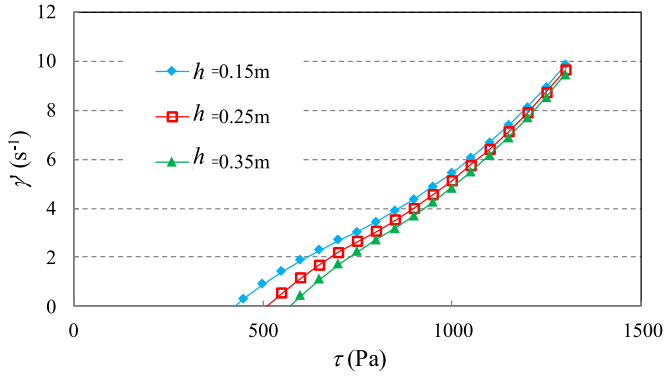

Fig. 6. The $\dot{\gamma}$ - τ relational curves of fresh concrete at different depths (h) (No. 1, t_0 = 0 s, $\Delta\tau$ = 50 Pa/s).

different depths within the range of the head of rod vibrator. The normal stress σ_n acting on the shear plane increases with the depth of concrete due to the increase of gravity. As shown in Fig. 6, the $\dot{\gamma}$ - τ relational curves go down with the increase of depth. That is to say, the concrete located in deeper position has greater shear deformation resistance. This is because the concrete located below has greater frictional resistance caused by the normal stress σ_n.

2.3. Effect of distance from vibrating source

The amplitude of internal vibrator operating in concrete is approximately 70 to 75% of its amplitude in air [1]. This is called load damping. Load damping coefficient (ζ_L) is expressed by Eq. (16) [20].

$$\xi_L = \frac{a'}{a} = \frac{m_v}{m_v + m_b}\left(\frac{f'}{f}\right) \tag{16}$$

where a' is acceleration of vibrator in concrete, a is acceleration of vibrator in air, m_v is mass of internal vibrator, m_b is mass of concrete removed by inserted vibrator, f' is frequency of vibrator in concrete, and f is frequency of vibrator in air.

However, the reduction of frequency in concrete is 1–3%. The ratio of f'/f is generally taken to be 0.98 [20]. Hence, the acceleration of vibrator in concrete is expressed by Eq. (17).

$$a' = \frac{0.98a \cdot m_v}{m_v + m_b} \tag{17}$$

In a homogeneous fluid, the amplitude generated around vibrating head will be the same as the inherent amplitude of vibrator. Fresh concrete, however, is not a homogeneous material. During vibration, cement paste will surround vibrator due to the liquefaction, which results in a reduction in energy transmission from the vibrator to fresh

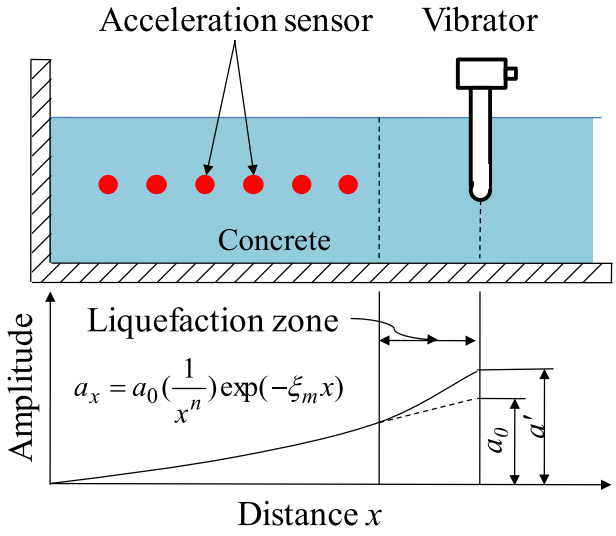

Fig. 7. Distance damping of vibration.

concrete [1]. This kind of damping is called boundary damping. The boundary-damping coefficient ($\zeta_B = a_0 / a'$, a_0 is the acceleration of vibrator actually applied to concrete) is dependent on the consistency of concrete. The greater the slump, the greater the damping, e.g. when the sump is 6 cm, and 11 cm, the ζ_B is 0.9, and 0.3, respectively [20]. However, now there is no predicting equation for the boundary damping.

Vibration intensity decreases gradually with the distance from vibrating source, as shown in Fig. 7. This kind of damping is called material damping or distance damping. The acceleration of vibration (a_x) at any distance (x) from vibrating source is expressed by Eq. (18).

$$a_x = a_0\left(\frac{1}{x^n}\right)\exp(-\xi_m x) \tag{18}$$

where x is distance from vibrating source, ζ_m is material damping coefficient, and n is geometric damping coefficient that is 0.5 in case of cylindrical vibrating source, and is zero in case of plane vibration wave.

Reference [20] shows that the material damping coefficient ζ_m is almost independent on vibrating time. The smaller slump, the greater the ζ_m. The ζ_m of concrete with 6 cm of slump is 0.04, but 0.01 for 11 cm of slump

Based on Eq. (17) and the boundary-damping coefficient, the acceleration of vibration in fresh concrete is obtained as Eq. (19).

$$a_x = \frac{0.98a \cdot m_v \cdot \xi_B}{m_v + m_b}\left(\frac{1}{x^n}\right)\exp(-\xi_m x) \tag{19}$$

The acceleration of vibration is a function of amplitude (S) and frequency (f), as shown in Eq. (19).

$$a = 4\pi^2 S f^2 \tag{20}$$

After substituting Eqs. (19) and (20) into Eqs. (14) and (15), and considering f'/f = 0.98, the shear deformation resistance of fresh concrete under vibration are expressed by Eqs. (21) and (22) for any vibrating time t and any horizontal distance x.

$$\tau = \sigma_n \tan\left\{(\phi_0 + \theta_0)\cdot\left[1 - \left[1 - \exp\left(-c_4 \frac{t}{x^{2n}\cdot\exp(2\xi_m x)}\right)\right]\right]\right\} + \eta\dot{\gamma} \tag{21}$$

when $c_2(\tau - \tau_{fd}) \leqq 1$

$$\tau = \sigma_n \tan\left\{(\phi_0 + \theta_0)\cdot\left[1 - \left[1 - \exp\left(-c_4 \frac{t}{x^{2n}\cdot\exp(2\xi_m x)}\right)\right]\right]\right\} + \frac{1}{c_2}\ln\dot{\gamma} \tag{22}$$

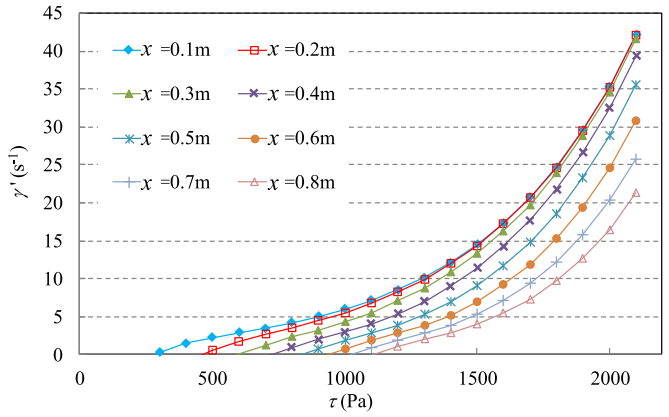

Fig. 8. Flow curves of vibrated concrete at different horizontal distances (No. 1, $t_0 = 0$ s, $\Delta\tau = 50$ Pa).

when $c_2(\tau - \tau_{fd}) > 1$where $c_4 = c_3\rho\left(\frac{0.98 \cdot \xi_B \cdot m_v \cdot a}{m_v + m_b}\right)^2/(16{\cdot}\pi^2{\cdot}(0.98f)^2)$

With the increase of distance x, the shear resistance τ increases for given concrete, vibrator, vibrating time, and shear rate. If x is enough large, the first term in the right of Eqs. (21) or (22) becomes to be $\sigma_n\tan(\phi_0 + \theta_0)$, thus there is no the effect of vibration.

Based on the parameters shown in Table 1, the consistency curves of fresh concrete No. 1 under vibration at different distances were gotten, as shown in Fig. 8. For the same shear stress, the shear strain rate decrease with the increase of distances. And the greater the distance x, the larger the decreasing degree. This is because that the vibrating energy damping happens in energy transmission, vibration force acting on fresh concrete decreases with the distance.

3. RSNS rheometer for dynamic measurement

3.1. Constitution of rheometer

As shown in Fig. 9, the RSNS rheometer consists of two separated cylindrical skirts with 340 cm of inside diameter, which were made of vinyl chloride. The upper skirt is fixed, and the upper blade can't rotate due to the impediment of the load cell. The lower blade was fixed to the lower skirt, and the lower skirt rotate by the drive of a motor. The gap between the two skirts is 3 mm, filled with mohair seal for preventing water and fine particle from leakage.

Two blades have 30 mm thick, were made of stainless steel, and are in radial pattern, as shown in Fig. 9(b), for avoiding the slip between the blades and concrete sample. The lower blade applies shear force to concrete above it through the concrete between the blade's spokes. And this structure also would permit the height of sample to increase freely but the shear thickness not to change. When fresh concrete is sheared, the dilatancy would occur [19], which results in a change of sample's height. According to the maximum size of coarse aggregate, the shear thickness of sample, that is to say, the interval between the two blades is set up within 50–250 mm in advance.

A rod vibrator, of which the diameter is 28 mm, the frequency is 220 Hz, and the amplitude is 1.8 mm, is used as the central motionless axis, thus fresh concrete is subjected to ring shear between two horizontal blades. In case of measuring the properties of fresh concrete under vibration, the vibrator works, otherwise it only acts as a fixed axis. Two air cylinders are arranged to this rheometer, by which a vertical force is applied to the aluminum plate that is placed on the top surface of concrete sample. Hence, the concrete sample must be filled above the upper blade. The cylinders can adjust the normal stress acting on the shear plane.

The RNSN rheometer is operated through a computer. The torque applied to the lower blade and the angle velocity of the lower blade is measured and controlled by a program installed into the computer. The rheological properties of fresh concrete under static state or vibration can be measured under torque growth method or rotation speed sweep control method. The measuring methods of rheological parameters of fresh concrete in static state and several measuring examples can be found in Ref. [15,16].

3.2. Calculations of shear stress, shear strain, and shear strain rate

Because there are frictional and slipping resistances at the inner wall of the upper skirt and the surface of rod vibrator, concrete sample is not in a sample shear state. Only part of the torque applied to the lower blade by the motor yields a shear deformation of concrete sample. According to the comparison of the numerical and experimental results, the frictional and slipping resistances have slight effect on the rheological test results of BTRHEOM [22]. And the diameter (340 mm) of sample of the RNSN rheometer is larger than that of the BTRHEOM rheometer, the effect of frictional and slipping resistances at the inner wall are less. The frictional and slipping resistances vary with concrete mixture, and we have no suitable method to predict them now. Therefore, we ignore them in this study.

The deformation in circumferential direction linearly increases from the surface of rod vibrator to the inner wall of the skirt, as shown in Fig. 10. The shear strain and shear strain rate in circumferential direction, of concrete at the top surface of the lower blade, are expressed by

$$\gamma = \frac{\pi r\varphi}{180h},\quad \dot{\gamma} = \frac{\pi r\Omega}{180h} \tag{23}$$

where, r is radius from the central of the upper skirt (mm), h is thickness of shear layer (mm) in vertical direction, and φ, Ω are rotation angle and angular speed, respectively.

Mean shear strain γ_m and mean shear strain rate $\dot{\gamma}_m$ occur in the middle circumference on the horizontal section of concrete, thus are expressed by Eq. (24)

$$\gamma_m = \frac{\pi(R_1+R_2)\varphi}{360h},\quad \dot{\gamma}_m = \frac{\pi(R_1+R_2)\Omega}{360h} \tag{24}$$

where R_1 and R_2 are respectively radius of the rob vibrator and the upper skirt.

The torque (Γ) acting on the horizontal section of concrete by the lower blade is calculated by Eq. (25).

$$\Gamma = \int_{R_1}^{R_2} 2\pi r^2\tau dr \tag{25}$$

where τ is shear stress at the circumference position of radius r.

Hence, the mean shear stress τ_m is calculated by Eq. (26).

$$\tau_m = \frac{3\Gamma}{2\pi(R_2^3 - R_1^3)} \tag{26}$$

If regarding fresh concrete as a Bingham fluid, shear stress linearly increases with the increase of the distance from the surface of the rod vibrator, thus mean shear stress τ_m occurs in the middle position, like as the mean shear strain rate. But for non-Newtonian and non-Bingham materials, the increase of shear stress is non-linear from the surface of rob vibrator to the inside wall of the upper skirt, thus the position of τ_m is unknown, depending on the τ -$\dot{\gamma}$ relational equation.

In theory, the shear deformation in circumferential direction increases with the radius of circumference, as shown in Eq. (23). However, for granular materials, e.g. soil, sand, and fresh concrete, the geometry and interlocking of particles causes the shear deformation in disorder. The particles, even initially subjected to large inter-particles forces, move slowly or shortly because their movements are restrained by standstill or slowly moving particles. Conversely, the particles, initially subjected to small inter-particles forces, are pulled so as to move rapidly or far. The movements of the particles deviate from their locating circumferences toward outermost circumference, as shown in

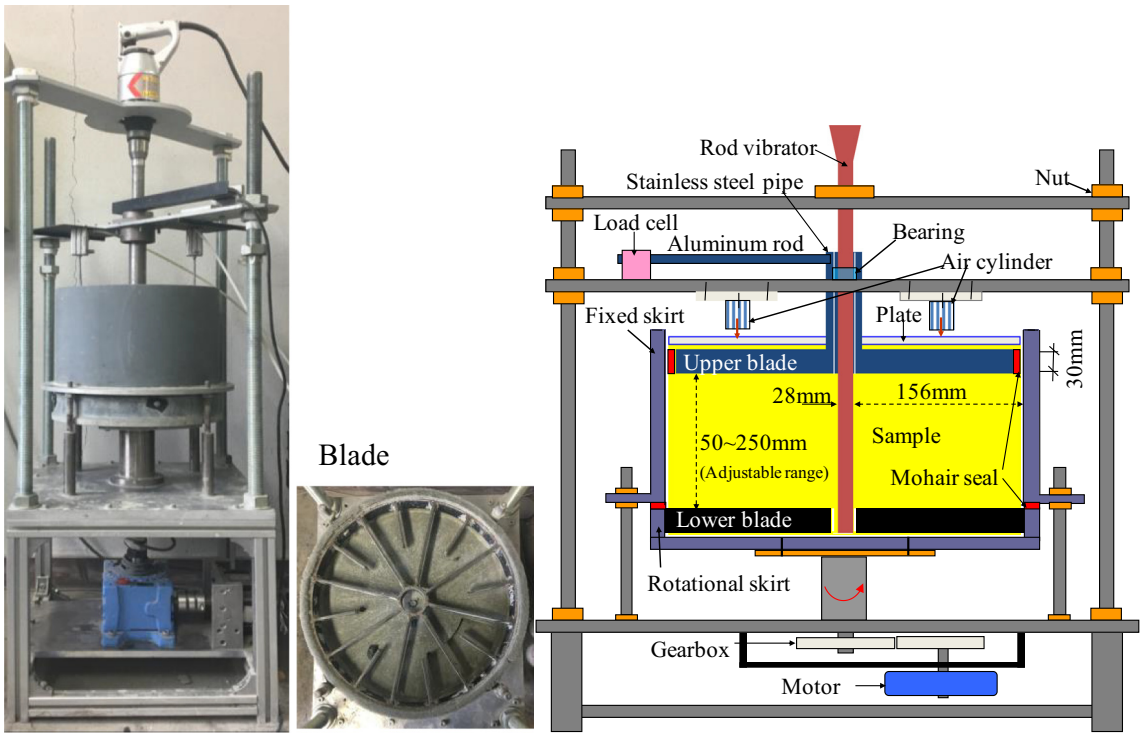

Fig. 9. RSNS rheometer.

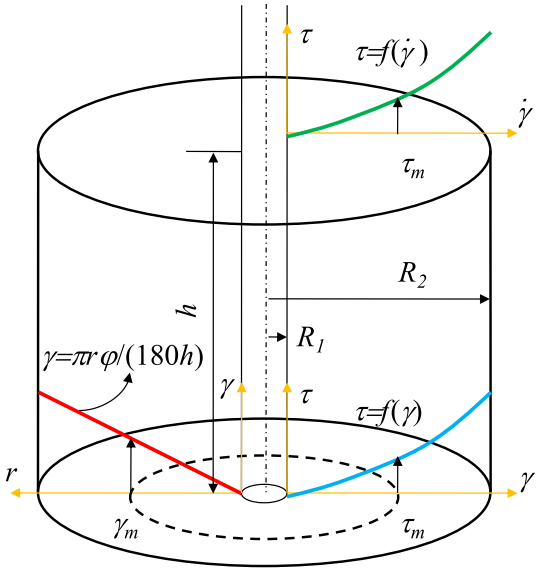

Fig. 10. Distribution of shear stress and shear strain rate in radial direction.

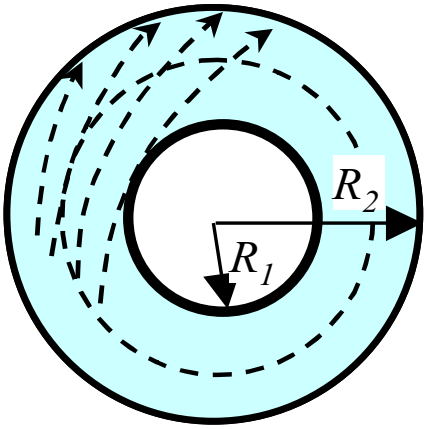

Fig. 11. Moving tracks of particles.

Fig. 11 [23]. Hence, the particles initially on different circumferences have near moving distance in the end, so-called harmonization effect. Because of the harmonization effect in particle movement, the stresses at different positions are near.

In case of soil, when the R_1/R_2 is over 0.5, the shear stress at the outmost circumference is almost equal to the mean stress in the range of R_1–R_2 [24], that is to say, the stress in the range of R_1–R_2 is almost changeless. The R_1/R_2 of the RSNS rheometer is < 0.5, but concrete has coarse aggregate particles, thus the harmonization effect is more remarkable. Now, we have no method to know the position where the mean shear stress (τ_m) occurs in the RSNS rheometer, but based on the above analysis, the supposition that the τ_m occurs at the middle of circumference like as the mean shear strain rate ($\dot{\gamma}_m$) has no great problem. In this study, we measured the τ_m-$\dot{\gamma}_m$ relationship of fresh concrete under vibration by using the RSNS rheometer to investigate experimentally the rheological behaviors of vibrated concrete.

4. Experimental program

4.1. Raw materials

Four series of fresh mortar and six series of fresh concrete were used. Mix proportions and slump values or table flow values are presented in Table 2. Ordinary Portland cement with specific surface area of 3500 cm^2/g and density of 3.16 g/cm^3 was used. Coarse aggregate was crushed siliceous stone with maximum diameter of 20 mm, density of 2.73 g/cm^3 in saturated surface dry state, water absorption rate of

Table 2
Mix proportions and fluidities of used mortars and concretes.

Series		W/C (%)	S/A (%)	SP/C (%)	Unit mass (kg/m³)					Sl. or f_t (cm)
					W	C	S	G	SP	
Mortar	M1	35	100	–	2342	669	1340	–	–	11.5
	M2	40	100		259	647	1293			16.8
	M3	45	100		282	625	1251			20.5
	M4	55	100		323	587	1174			20.8
Concrete	C1	40	38.9	0.50	170	425.0	668	1067	2.1	13.5
	C2	45	40.0	0.75	170	377.8	706		1.9	17.5
	C3	55	41.9	0.50	170	309.1	762		1.5	16.3
	C4	45	40.8	0.50	165	366.7	728		1.8	17.0
	C5	45	39.1	0.50	175	388.9	684		1.9	19.0
	C6	45	38.5	0.50	180	400.0	662		2.0	19.8

[Notes] *W*: water, *C*: ordinary Portland cement, *S*: sea sand: *G*: crushed stone, *SP*: high range AE water-reducing agent, *W/C*: water-cement ratio, *S/A*: fine-aggregate ratio by mass, *SP/C*: SP dosage by mass, *Sl.*: slump of concrete, and f_t: flow table value of mortar.

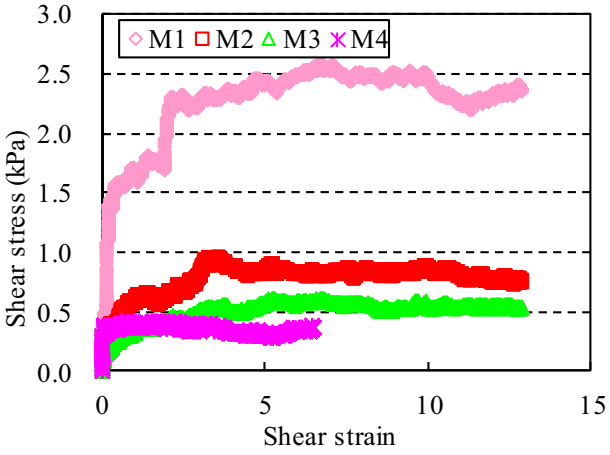

Fig. 12. Relationship of shear stress and shear strain of fresh mortar in vibrated state.

0.47%, solid volume percentage of 59.2%, and fineness modulus of 6.68, respectively. Fine aggregate was sea sand with density of 2.57 g/cm³ in saturated surface dry state, water absorption rate of 1.36%, solid volume percentage of 66.7%, and fineness modulus of 2.90, respectively. Retarding type-high range AE water-reducing agent was added in the concrete mixtures. Series M1–M4 of mortar and Series C1–C3 of concrete had different water-cement ratios by mass. Series C4–C6 of concrete had different unit water contents.

18 l of mortar or concrete sample was prepared by a concrete mixer. The cement and fine aggregate were first put into the mortar or concrete mixer, and mixed for 1 min. Then water and the admixture were added and further mixed for 2 min. In the case of concrete, coarse aggregate was finally added and mixed for another 2 min. Right after mixing, the slump test and the air content test of concrete or the flow table test of mortar were performed.

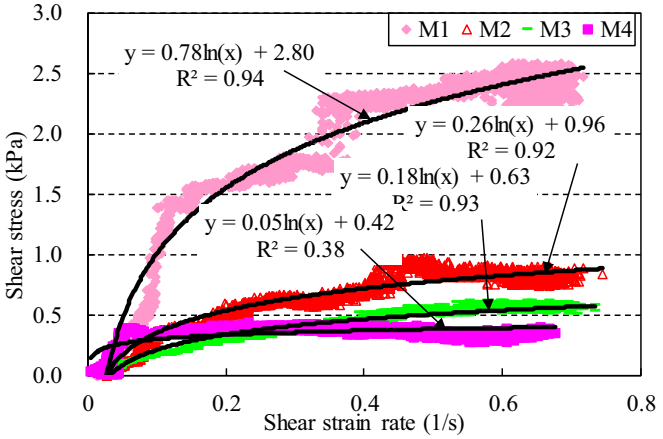

Fig. 14. Relationship of shear stress and shear strain rate of fresh mortar in vibrated state.

4.2. Procedure of rheological test

The shear thickness of sample in vertical direction was 100 mm. After the mortar or concrete sample was filled into the two skirts of the RSNS rheometer. Vibration was added by using the rod vibrator of the rheometer for 5 s to guarantee that the rod vibrator closely contacts the sample. Even so, the turbulence in initial measurement may occur since the contacts between the two blades and sample are not always close. Therefore, for making the contacts close to get stable test results, in unvibrated state, the torque was increased by a load speed of 0.1 N·m/s until corresponding angular speed of the lower blade exceeded 5 deg./s.

Once the angular speed of the lower blade reached to 5 deg./s, the measurement under vibration was atomically started. The angular speed of the lower blade was increased from 5 to 45 deg./s at a rate of 2 deg./s². The angular speed, rotational angle and torque of the lower blade as well as the torque of the upper blade were record in an interval of 0.1 s by a data logger and the computer. Mean shear strain, mean shear rate and mean shear stress are calculated by Eqs. (24) and (26), respectively. Vibration may result in segregation of fresh mortar or fresh concrete to affect the experimental results of shear stress – shear strain/shear strain rate relationships. For avoiding the effect of segregation, we measured the shear stress - shear strain/shear strain rate relationships just within a few seconds from the beginning of vibration.

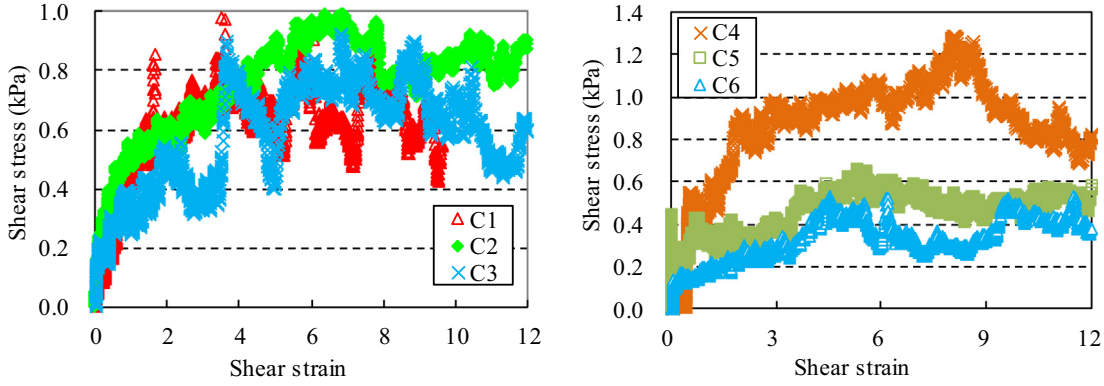

Fig. 13. Relationship of shear stress and shear strain of fresh concrete in vibrated state.

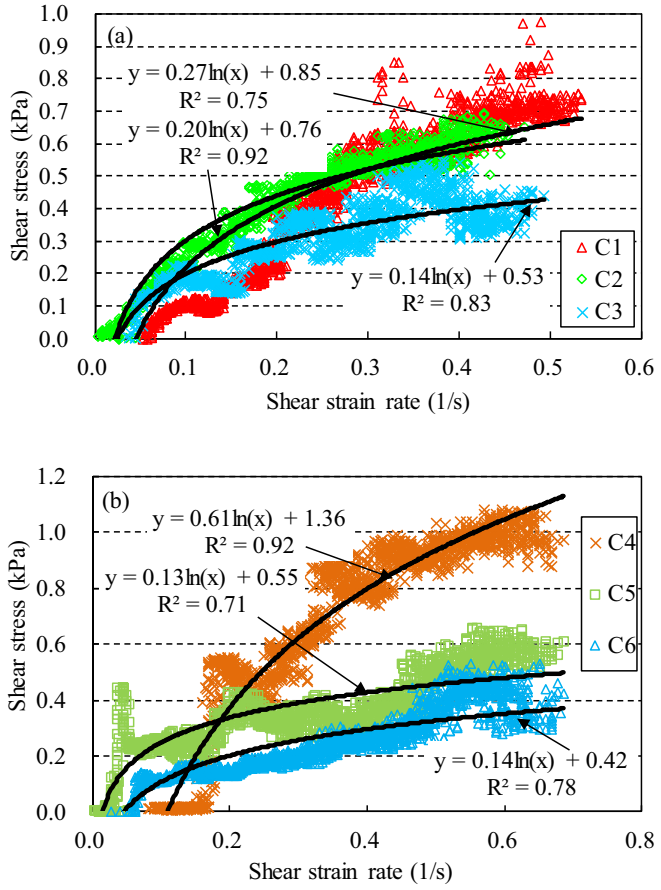

Fig. 15. Relationship of shear stress and shear strain rate of fresh concrete ((a) C1–C3, (b) C4–C6) in vibrated state.

The rotating angle of the lower blade was < 90 deg. Once we found the shear stress increased abnormally, we stopped the measurement.

5. Test results and discussion

Figs. 12 and 13 show the relationship of mean shear stress (τ_m) τ and mean shear strain (γ_m) of fresh mortar and fresh concrete in vibrated state, respectively. No matter what kind of sample, with the increase of γ_m, the τ_m increased rapidly in the beginning, then decreased very slowly after it reached to a peak. It is considered that after the peak of shear stress, the sample entered into shear failure, and the shear deformation decreases gradually. Moreover, from Figs. 12 and 13, we found that greater water-cement ratio or water content causes the shear deformation to decrease for a given shear strain.

The change of τ_m with mean shear strain rate ($\dot{\gamma}_m$) of fresh mortar and fresh concrete under vibration is shown in Figs. 14 and 15. The τ_m-$\dot{\gamma}_m$ relational curves were measured simultaneously when the vibration started. As shown in Figs. 14 and 15, the measured τ_m-$\dot{\gamma}_m$ relational curves are non-liner, and their starting points are very near the origin of coordinates. The τ_m increased with the increase of the $\dot{\gamma}_m$. The regressive analyses toward the whole τ_m-$\dot{\gamma}_m$ relational curves were done, as shown in Figs. 14 and 15. We found that the τ_m is a logarithmic function of $\dot{\gamma}_m$, which agrees with the Eq. (11). However, in the range of low shear strain rate, the experimental data deviate the logarithmic curves.

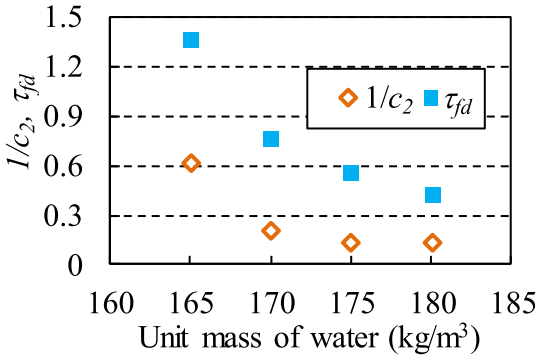

Fig. 17. The effects of water content on the $1/c_2$ and τ_{fd} of fresh concrete (Series C2, C4–C6).

Figs. 16(a) and (b) show the changes of rheological parameters: $1/c_2$ and τ_{fd} in Eq. (11) with water-cement ratio (W/C) of the fresh mortars (Series M1-M4) and the fresh concretes (Series C1–C3), respectively. Also, Fig. 17 shows the effect of water content on the two rheological parameters of the fresh concretes (Series C2, C3–C6). Since the τ_{fd} changes with vibrating time, the τ_{fd} gotten through the regressive analysis shown in Figs. 4–16 is actually an apparent value. For both fresh mortar and fresh concrete, the $1/c_2$ and the τ_{fd} decreased with the increase of W/C. The $1/c_2$ and the τ_{fd} of fresh concrete decreased with increasing unit mass of water.

6. Conclusions

For clarifying the constitutive model of fresh concrete in vibrated state, the theoretical analysis of rheological behavior of fresh concrete was firstly performed on basis of the viscosity theory of Eyring rate process. The effects of vibrating time and vibration damping with distance from vibrator were taken into account. The rheological model of fresh concrete in vibrated state was proposed.

At low shear strain rates, fresh concrete under vibration is a Bingham liquid. With the increase of vibrating time, the yield stress decreases, but the apparent viscosity increases for a given shear strain rate. If the vibrating time is enough long, vibrated fresh concrete is nearly Newtonian. However, at high shear strain rates, the shear stress (τ) – shear strain rate ($\dot{\gamma}$) relationship is a logarithmic function or an exponential function. The shear deformation resistance decreases with increasing vibrating time, but increases with the distance from

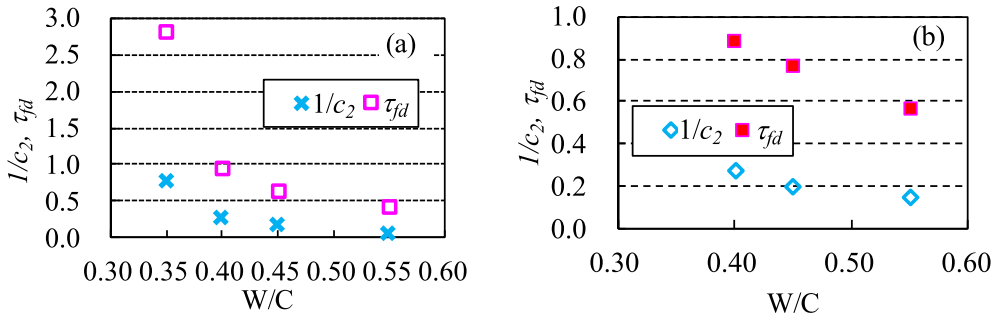

Fig. 16. The effects of water-cement ratio (W/C) on the $1/c_2$ and τ_{fd} of (a) fresh mortar and (b) fresh concrete (Series C1–C3).

vibrating source. For given vibrating time and shear strain rate, the shear deformation resistance of concrete under vibration increases with depth due to the increase of vertical stress acting on shear plane, which is caused by concrete's gravity. The elapsed time of vibration before rheological measurement, and increasing speed of shear stress greatly affect the measuring result of the $\tau - \dot{\gamma}$ relational curve. The longer the elapsed vibrating time or the smaller the increasing speed, the smaller shear deformation resistance for a given shear strain rate.

Rheological measurement of fresh mortar and fresh concrete in vibrated state was also conducted by using a ring shear type rheometer, into which a rod vibrator was integrated. The experimental results of $\tau - \dot{\gamma}$ relationship were consistent with the theoretical equations very well. And we found that the rheological parameters τ_{fd}, $1/c_2$ in Eq. (11) decrease with increasing water-cement ratio or water content of fresh concrete.

References

[1] A. C. 309, Report on Behaviour of Fresh concrete During Vibration, American Concrete Institute, Detroit, ACI 309.1R-08 (2008).
[2] M.I. Safawi, I. Iwaki, T. Miura, The segregation tendency in the vibration of high fluidity concrete, Cem. Concr. Res. 34 (2) (2004) 219–226.
[3] R. W. Taylor, The compaction of concrete by internal vibrators-an investigation of the effects of frequency and amplitude, Technical Report No 42.511, Cement and Concrete Association, Slough in, 1976.
[4] P. Banfill, M. Teixeira, R. Craik, Rheology and vibration of fresh concrete: predicting the radius of action of poker vibrators from wave propagation, Cem. Concr. Res. 41 (9) (2011) 932–941.
[5] H. Mori, Y. Tanigawa, Flow simulation of fresh concrete subjected to vibration, Mag. Concr. Res. 42 (153) (1990) 223–232.
[6] Z. Li, T. Ohkubo, Y. Tanigawa, Yield model of high fluidity concrete in fresh state, J. Mater. Civ. Eng. 16 (3) (2004) 195–201.
[7] R.L. Hemite, G. Tournnon, Vibration of Fresh Concrete, John Wiley & Sons Inc., 1968, pp. 501–503.
[8] Z. Li, Y. Tanigawa, Investigation on granular characteristics of fresh concrete based on visualized experiment using alternative materials, Journal of Structural and Construction Engineering, Transaction of Architectural Institute of Japan 77 (678) (2012) 1175–1184.
[9] A. Committee, Behaviour of Fresh Concrete During Vibration, (2010).
[10] G. Tattersall, P. Baker, The effect of vibration on the rheological properties of fresh concrete, Mag. Concr. Res. 40 (143) (1988) 79–89.
[11] G. Tattersall, P. Baker, An investigation on the effect of vibration on the workability of fresh concrete using a vertical pipe apparatus, Mag. Concr. Res. 41 (146) (1989) 3–9.
[12] K. Teranishi, Study on dynamic model of Bingham's fluid subjected to vibration, Journal of Structural and Construction Engineering, Transactions of Architectural Institute of Japan, (467) (1995) 1–8.
[13] C. Hu, F. de Larrard, The rheology of fresh high-performance concrete, Cem. Concr. Res. 26 (2) (1996) 283–294.
[14] Z. Li, T. Ohkubo, Y. Tanigawa, Flow performance of high-fluidity concrete, J. Mater. Civ. Eng. 16 (6) (2004) 588–596.
[15] Z. Li, Rheological model and rheometer of fresh concrete, Journal of Structural and Construction Engineering, Transaction of Architectural Institute of Japan 80 (710) (2015) 527–537.
[16] G. Cao, Z. Li, Numerical flow simulation of fresh concrete with viscous granular material model and smoothed particle hydrodynamics, Cem. Concr. Res. 100 (2017) 263–274.
[17] Z. Li, Theoretical investigation on rheological properties of fresh concrete, Journal of Structural and Construction Engineering, Transaction of Architectural Institute of Japan 78 (687) (2013) 895–904.
[18] J. Li, Z. Li, Effect of boundary restraint on the flow of fresh concrete through opening, Journal of Structure and Construction Engineering, Transaction of Architectural Institute of Japan 76 (666) (2011) 1367–1374.
[19] Z. Li, J. Li, Granular material characteristic of fresh concrete, Proceedings of 6th International RILEM Symposium on Self-Compacting Concrete, 2010, pp. 423–433.
[20] N. Murata, Science and Technology of Concrete, Sankaido Publishing Co., Ltd., 1996, pp. 120–132.
[21] Z. Li, T. Ohkubo, Y. Tanigawa, Theoretical analysis of time-dependence and thixotropy of fluidity for high fluidity concrete, J. Mater. Civ. Eng. 16 (3) (2004) 247–256.
[22] C. Hu, F. de Larrard, T. Sedran, et al., Validation of BTRHEOM, the new rheometer for soft-to-fluid concrete, Mater. Struct. 29 (10) (1996) 620–631.
[23] S. Osano, Direct shear box and ring shear test comparison: why does internal angle of friction vary, ICASTOR Journal of Engineering 5 (2) (2009) 77–93.
[24] T.D. Stark, I.A. Contreras, Constant volume ring shear apparatus, Geotech. Test. J. 19 (1) (1996) 3–11.